Title: A morphometric study of mechanotransductively induced dermal neovascularization.
Authors: Erba P, Miele LF, Adini A, Ackermann M, Lamarche JM, Orgill BD, D'Amato RJ, Konerding MA, Mentzer SJ, Orgill DP
Journal: Plastic and reconstructive surgery
Year: 2011 Oct
Volume: 128
Issue: 4
Pages: 288e-299e
DOI: 10.1097/PRS.0b013e3182268b19

Published in final edited form as:
Plast Reconstr Surg. 2011 October ; 128(4): 288e–299e. doi:10.1097/PRS.0b013e3182268b19.

A Morphometrical Study of Mechanotransductively Induced Dermal Neovascularization

Paolo Erba, MD[1,2], **Lino F Miele, MD**[4], **Avner Adini, PhD**[3], **Maximilian Ackermann, MD**[5], **James M Lamarche**[1], **Britlyn D Orgill**[1], **Robert J D'Amato, MD, PhD**[3], **Moritz A Konerding, MD**[5], **Steven J Mentzer, MD**[4], and **Dennis P Orgill, MD, PhD**[1]

[1]Tissue Engineering and Wound Healing Laboratory, Division of Plastic Surgery, Brigham and Women's Hospital, Harvard Medical School, Boston, MA, USA [2]Department of Plastic, Reconstructive and Aesthetic Surgery, University Hospitals of Basel and Lausanne, Switzerland [3]Department of Surgery, Vascular Biology Program, Harvard Medical School, Children's Hospital Boston, Boston, MA, USA [4]Laboratory of Adaptive and Regenerative Biology, Department of Surgery, Brigham and Women's Hospital, Harvard Medical School, Boston, MA [5]Institute of Functional and Clinical Anatomy, University Medical Center of the Johannes Gutenberg-University Mainz, Germany

Abstract

Background—Mechanical stretch has been shown to induce vascular remodeling and increase vessel density, but the pathophysiological mechanisms as well as the morphological changes induced by tensile forces to dermal vessels are poorly understood.

Methods—A custom computer controlled stretch device was designed and applied to the backs of C57BL/6 mice (n=38). Dermal and vascular remodeling was studied over a 7 days period. Corrosion casting and three-dimensional (3D) scanning electron microscopy (SEM) as well as CD-31 staining were performed to analyze microvessel morphology. Hypoxia was assessed by immunhistochemistry. Western blot analysis of VEGF and mRNA expression of VEGF receptors were performed.

Results—Skin stretching was associated with increased angiogenesis as demonstrated by CD31 staining and vessel corrosion casting where intervascular distance and vessel diameter were decreased ($p<0.01$). Immediately after stretching VEGF dimers were increased. mRNA expression of VEGFR1, VEGFR2, NP1 and NP2 were increased starting as early as 2 hours after stretching. Highly proliferating epidermal cells induced epidermal hypoxia starting at day 3 ($p<0.01$).

Conclusion—Identification of significant hypoxic cells occurred after identification of neovessels suggesting an alternative mechanism. Increased expression of angiogenic receptors, stabilization of VEGF dimers may be involved in a mechanotransductive, prehypoxic induction of neovascularization.

Address for correspondence: Paolo Erba, MD, Department of Plastic, Reconstructive and Aesthetic Surgery, University Hospital of Lausanne, CH-1011 Lausanne, Switzerland, Tel: +41 79 556 32 23, Fax: +41 21 314 25 31, erbapaolo@hotmail.com.
Dr. P. Erba and Dr. L.F. Miele equally contributed to this publication.

Conflict of Interest
The authors state no conflict of interest.

Financial Disclosure
None of the authors have any financial interest that might pose or create a conflict of interest with the information presented in this manuscript.

Introduction

Mechanical forces influence physiological and pathological tissue development and neovascularization. There is an increasing interest of scientists and clinicians in better understanding the mechanobiological processes controlling angiogenesis in living tissues [1,2]. Micromechanical deformations are known to induce the expression of angiogenic growth factors and receptors such as vascular endothelial growth factor (VEGF), VEGF receptors and angiopoietin system receptors [3–6]. In vitro endothelial cell stretching leads to increased new vessel formation [7–8]. Previously we showed that tensile forces induce cell proliferation and vascular tissue growth in the skin of a rat ear [9]. Several research groups found an increased expression of VEGF following the application of cyclical stretch forces [10,11]. By gene chip analysis and RT-PCR, we previously identified a possible relationship between stretch-induced vascular remodeling and increased expression of HIF-1α [9,12,13]. Because expression and degradation of HIF-1α are regulated by oxygen dependent proxyl hydroxylases and proteosomal degradation mechanisms [14], these findings suggest that increased expression of HIF-1α and related angiogenic factors such as VEGF may be regulated by changes in tissue oxygenation following skin stretch. Petersen et al. identified that in tendon fibroblasts, stretch induces the expression of selected VEGF isoforms [15]. Different patterns and forms of applied mechanical forces could therefore influence angiogenesis through the formation of secondary VEGF structure with increased biological function.

Using corrosion casting and scanning electron microscopy techniques we aimed to study the morphometrical characteristics of stretching-induced dermal neovascularization and attempted to investigate how epidermal proliferation, hypoxia, and induced expression of VEGF affect microvascular remodelling in response to stretch-induced mechanical force.

Materials and Methods

Thirty-eight adult male wild-type C57BL/6 mice (Jackson Laboratory, Bar Harbor, ME) were included in this study. Mice were housed in an Association for Assessment and Accreditation of Laboratory Animal Care certified facility under an approved experimental protocol. The entire dorsum of the animals was clipped and depilated (Nair®, Church & Dwight Co., Princeton, NJ) 24 hours prior to the beginning of each experiment. Animals were anesthetized with 60 mg/kg Nembutal (Pentobarbital) 15 minutes prior application of the stretching device. The feet of stretching device were positioned 1 cm apart and fixed to the skin of the dorsum using cyanoacrylate glue. Skin was then stretched in the cranio-dorsal direction for 4 hours with a static stretching pattern. This treatment time was determined to be the longest period of stretching applicable to our model without causing skin damage to the studied mice. At the end of the stimulation, the device was carefully detached from the mouse. All animals were caged separately and allowed to freely move in their cages with water and food ad libitum. In order to study the time changes of stretch-induced dermal and microvascular remodeling, animals were euthanized at 2 hours (n=6), 3 days (n=6) and 7 days (n=20) after stretching. The stretched skin area was then divided into two parts. The caudal part was used for immunhistochemistry studies, and the cranial part was equally divided and used for western blot analysis and real time RT-PCR (n=3 per group). Stretched skin samples were compared to tissues harvested from control animals with non-stretched skin (n=6). Fourteen of the animals harvested at day 7 were used for corrosion casting analysis of skin vessels.

Stretch Device

The computer-controlled device consisted of an ultra lightweight distractor moving via a closed pneumatic system powered by a stepper motor (43F4(5)-Q, Haydon Switch and

Instruments Inc, Waterbury, CT), which was coupled with a control unit (DCS4020 bipolar chopper, Haydon Switch and Instruments Inc, Waterbury, CT) and a data acquisition unit (NI USB-6008, National Instruments, Plano, TX). The distractor was made from a lightweight ABS plastic and weighed less than 10 g allowing animals to move and eat ad libitum during the experimental procedure, which was not possible with previously used machines. The device could deliver constant force with a resolution of 0.1N. The machine self-corrected if the measured forces on the animal deviated from the user determined range, which was necessary as air leaks were inevitable in the pneumatic system. To further ensure the accuracy of the device, a calibration function was implemented. Labview 8.6 (National Instruments Corp., Austin, TX) was used for data acquisition and closed loop force control of the distractor allowing instant feedback of the force readings being applied to the animal.

Corrosion Casting

For spatial visualization of dermal microvasculature, 14 mice were euthanized on day 7. After systemic heparinization, mice were euthanized with ketamine 120mg/kg and Xylazine 5 mg/kg and via the left ventricle the system was first flushed with 20 mL PBS (Mediatech, Inc., Herndon, VA) and then perfused with 5 mL 2.5% Glutaraldehyde (Electron Microscopy Sciences, Washington, PA) warmed to 35°C. The right atrium was vented. 15 mL PU4ii (vasQtec, Zurich, Switzerland) mixture was subsequently infused. The skin was harvested and placed in 7.5% KOH (Sigma-Aldrich Co., St. Louis, MO) at 40°C until fully corroded. The specimens were dehydrated, mounted on conductive stubs and coated with gold in an SCD 040 sputter-coater (BAL-TEC AG, Leica Microsystems) and visualized under a Philips XL30 scanning electron microscope (Philips, Eindhoven, The Netherlands). Between 20 and 30 stereo pair images with a 61° tilt angle were recorded per sample and analyzed with the image analysis program, Kontron KS 300 (Carl Zeiss Vision, Eching, Germany), to calculate the parameters associated with microvascular architecture, such as the intervascular and interbranch distances and microvascular diameter variation. For details see Erba et al. (2010) [16] and Malkusch et al. (1995) [18].

Immunohistochemistry of Skin Vasculature, Epidermal Proliferation and Hypoxia

Skin, underlying subcutaneous tissue, and panniculus carnosus muscle were harvested, formalin-fixed and embedded in paraffin. Analysis of skin vasculature, epidermal proliferation and hypoxia was performed by immunohistochemistry as previously described [16]. CD31 (Pharmingen, San Jose, CA), Ki-67 (LabVision, Freemont, CA) and anti-Hypoxyprobe™-1 monoclonal antibody (NPI, Burlington, MA) were used. Isotype-matched antibody controls were performed. Six digital images of stained cross sections were captured for each sample. Blood vessel density was quantified as the ratio of blood vessel number per high-powered field (hpf). Cellular proliferation was quantified as the ratio of Ki-67 positive cells to the total number of nuclei present in the basal layer of the epidermis. Epidermal hypoxia was quantified as the ratio of total number of positive cells to the total number of cells in the epidermis. A total of 30 microscopic fields for each experimental group were evaluated by three blinded observers.

Immunhistochemistry of Epidermal Thickness

Paraffin embedded tissues were sectioned and stained according to routine Hematoxylin and Eosin (H&E) protocols. Epidermal thickness was measured by counting the layers of cells composing the epidermis as well as by counting the number of cells composing each layer so the total number of cells in the image could be calculated.

Western Blot Analysis of VEGF

In order to assess the protein level of VEGF, skin harvested from the same animals used for RT-PCR studies was harvested and fresh frozen (n = 3 per group). The samples were loaded on 15% SDS–polyacrylamide gel and run at 120V for 90 minutes. The protein was transferred to PVDF membrane and subsequently blocked for 2 hours with 10% milk in TBST (10mM Tris base pH 7.5, 150mM NaCl, 0.1% Tween-20). The membrane was then incubated in primary polyclonal antibody against VEGF. Following three washes with TBST for 10 minutes each, the membrane was placed in the secondary goat-anti-rabbit antibody (Rockland Immunochemicals Inc., Gilbertsville, PA, USA) for 1 hour. The enhanced chemiluminescence reaction (ECL, Amersham Biosciences, Iscataway, NJ, USA) was then carried out according to the manufacturer's instructions, and films were developed for 30 seconds with phosphatase-conjugated secondary antibody.

Real Time RT-PCR Analysis of Angiogenic Receptors

Real-time RT-PCR expression of vascular endothelial growth factor receptor 1 (VEGFR1) and 2 (VEGFR2), neuropilin receptor 1 (NP1) and 2 (NP2) was performed for tissues harvested 2 hours, 3 days and 7 days after stretching and compared with samples harvested from non-stretched animals (n = 3 per group). Control and stretched samples were homogenized manually in 1.5 ml RNAase-free microfuge tubes (Ambion, Austin, TX). RNA was extracted from the homogenate using the Trizol reagent (Invitrogen, Carlsbad, CA) and treated with DNA-free reagents and protocols provided by the manufacturer. RNA yield was measured and reverse transcription of the 1 μgRNA template was performed using AffinityScript QPCR cDNA Synthesis Kit (Stratagene, La Jolla, CA) on a PTC-200 thermal cycler (MJ Research). Duplex real-time PCR reaction was conducted in 96-well format with 20ul reaction volume. Each well contained 1 μl each of cDNA, 1 μl of probe primers (Applied Biosystems, Foster City, CA), 1 μl of endogenous control primers, 10 μl of Taq man, a universal PCR master mix (Applied Biosystems Foster City, CA). Applied Biosystems mouse 18S RNA- VIC probe was used as the endogenous control and the tested probes were: prom1 (Mm00477115_m1), VEGFR1 (Mm00438980_m1), VEGFR2 (Mm00440102_m1) Neuropilin 1 (Mm00435379_m1) and Neuropilin 2 (Mm00803101_m1). Quantitative PCR was performed on a MX3005P Real-Time PCR system using built-in comparative quantification software and protocol (MxPro, Stratagene). All samples were conducted in triplicates and data analysis was conducted using MxPro. 18S and 28 S have been proved to be the most reliable internal control for comparative analyses of transcription under hypoxic conditions [19]. Change in expression was considered significant when the baseline relative quantity (RQ) minimum/maximum values did not overlap with the sample RQ values at the 95% confidence interval determination.

Data Analysis

Statistical analyses and graphic displays were performed using Sigmaplot and SPSS software (Chicago, IL, USA). Statistical significance was evaluated using the Mann–Whitney and Student's t-tests. A p-value less than 0.05 was considered statistically significant.

Results

Stabilization of VEGF dimers is associated with neovascularisation in stretched skin (Figure 1–4)

VEGF protein measurements assessed by western blot analysis showed reduced VEGF monomers and increased VEGF dimers immediately after stretching suggesting a possible stabilisation of the dimers mediated by mechanical forces. Slightly increased levels of

VEGF were found starting at day 3 and remained elevated for the whole observation time of 7 days (Figure 1). Stabilization of VEGF dimers was associated with neovascularization of stretched skin as confirmed by CD31 stained sections where starting at 3 days after stretching, there was an increasing number of capillaries (Figure 2). Compared to scanning electron microscopy images of corrosion casts of control skin samples, stretched skin presents with densely packed thin vessel bundles in the surrounding of the stretched skin area. In the stretched skin area, an angiogenic transition zone with tortuous elongated and dilated vessel bundles is found. Decelerated blood flow and angiogenesis in the transition zone is responsible for the formation of microvascular sprouts and sinusoids [20]. Stretched skin microvessels had a decreased intervascular distance ($p<0.001$) indicating greater vessel density compared to controls. Vessel diameter was found to be smaller in stretched skin ($p<0.01$) compared to control skin.

Skin stretching leads to a modulation of the expression of mRNA of angiogenic receptors (Figure 1)

Skin stretching induced a modulation of the expression of VEGF Receptors. mRNA expression of VEGFR1, VEGFR2 and NP1 showed only a moderate increase starting as early as 2 hours after stretching and reaching an expression peak at day 3. The mRNA expression levels of these receptors returned to the levels of non-stretched skin at day 7. The expression of Neuropilin 2 receptor was highly affected by stretching, showing a 4 fold increase already 2 hours after stretching and reaching a 12 fold of its original level 7 days after stretching.

Skin Stretching leads to immediate epidermal cell proliferation. Highly proliferative cells may be the cause of increasing epidermal hypoxia starting at day 3 and peaking at day 7 (Figure 5)

Skin cross sections of unstretched animals present with sporadic Ki-67 positive cells located in the basal layer of the epidermis. As soon as 2 hours after stretching, there is a 5 fold increase of positive cells, which remain at comparably high levels over the entire observation period of 7 days. Highly proliferating cells lead to a thickening of the epidermis. Non-stretched skin presents with an average of 18 ± 2 cells per high power field and up to 2 cell layers. The number of epidermal cells and the number of cell layers increase to 38 ± 10, to 4 layers respectively 7 days after stretching. Along with increasing cell proliferation and epidermal thickening, pimonidazole hydrochloride marker accumulates in an increasing number of cells, which are primarily at the surface of the epidermis. While hypoxia was nearly absent during active stretching (2 ± 2 % positive cells per hpf), in non-stretched skin (2 ± 1 % positive cells per hpf) and at 2 hours after stretching (19 ± 7 % positive cells per hpf), hypoxic cells started to appear at day 3 (30 ± 11 % positive cells per hpf) and hypoxia became evident at day 7 (45 ± 8 % positive cells per hpf, $p<0.01$), where several epidermal layers were positively stained. Compared to non-stretched animals, seven days after stretching the number of hypoxic cells presented with a 28 fold increase.

Discussion

Conventional tissue growth strategies such as tissue expansion and distraction osteogenesis rely on the static application of mechanical forces [21–23]. A better understanding of how static tensile forces modulate tissue growth and angiogenesis is important in order to optimize and develop novel devices and tissue engineering therapies that rely on mechanical forces.

Consistent with previous reports, we demonstrated that mechanical forces produced by stretching leads to increased tissue angiogenesis. Corrosion casting analysis of stretch-

induced neovessels demonstrated how stretched skin results in a decrease in intervascular distance and an increase in vessel density. Angiogenic foci not present in control animals were found in the stretched skin regions and were characterized by a transition zone with multidirectional microvascular sprouts and sinusoidals. Surrounding the foci, stretched skin presented with a region of densely packed vessel bundles which ensured optimal perfusion to this angiogenic transition zone [24].

Gene chip analysis and RT-PCR analysis performed by our group on stretched rat ear tissue suggested however that HIF-1α plays a role in mechanically-induced vascular remodelling [12]. Because expression and accumulation of HIF-1α is regulated by oxygen dependent mechanisms [14], we initially hypothesized that modulation of tissue oxygenation might occur during active stretching. More precisely we hypothesized that hypoxia might have occurred temporarily during stretch, thereby stimulating the expression of HIF-1α and dependent angiogenic factors. To test this hypothesis we used pimonidazole hydrochloride as an in vivo marker for hypoxic cells. Pimonidazole competitively binds for oxygen molecules in cells that have oxygen tension less than 10 mmHg [25,26] and has been proven to be a reliable marker of cutaneous hypoxia [27,28]. However, we found that the number of hypoxic cells was negligible during active stretching as well as 2 hours after stretching but that it was clearly increased starting at day 3 in parallel to an increase in epidermal thickness. We therefore conclude that skin is not hypoxic during active stretching but that hypoxia occurs later, probably as a consequence of highly proliferating cells with an increased demand of nutrients and oxygen supply. Hypoxia seems therefore not to be related to the rapidly increased expression of HIF1-α. In order to investigate if other mechanisms different from hypoxia may be responsible for the regulation of vascular remodeling of stretched skin, we investigated the mRNA expression of VEGF receptors as well as VEGF dimerization. As previously described in a study with negative pressure wound therapies [16], the application of mechanical forces to dermal tissues may be associated with the increased stabilisation of VEGF dimers. VEGF dimers have been recognized to have a superior biological function and to lead to a more effective angiogenesis [29,30]. In our experiments we observed that in the 2 hours group VEGF degradation to monomers was dramatically reduced while VEGF dimers had almost doubled. Besides an improved stabilisation of VEGF dimers, it is possible that VEGF monomers bind to dimers under the effect of mechanical stretching forces and thereby lead to an increased angiogenesis. VEGF dimers normalized at day 3 and day 7 suggesting that dimerization occurs immediately as a direct effect of tensile forces. Also the increased expression of angiogenic receptors, especially NP2 could be involved in a mechanotransductive, prehypoxic induction of neovascularization.

These results provide important insights for the understanding of stretching induced vascular remodelling, a complex process consisting in the coordinated expression of angiogenic factors and receptors, modulation of tissue oxygenation as well as the direct effect of mechanical forces on living tissues. The use of tensile forces for tissue engineering purposes will require further studies to determine the trade-off between tissue injury and tissue response. Besides improving our understanding on tissue and species dependent factors affecting the balance between tissue injury and tissue response, we propose the selection of different patterns of stretching in order to optimize this trade-off. A cyclical pattern of tensile forces could achieve comparable tissue responses allowing a periodic tissue recovery and thereby minimizing tissue injury.

References

1. Butcher DT, Alliston T, Weaver VM. A tense situation: forcing tumour progression. Nat Rev Cancer. 2009; 9:108–122. [PubMed: 19165226]

2. Kilarski WW, Samolov B, Petersson L, et al. Biomechanical regulation of blood vessel growth during tissue vascularization. Nat Med. 2009; 15:657–664. [PubMed: 19483693]

3. Li J, Hampton T, Morgan JP, et al. Stretch-induced VEGF expression in the heart. J Clin Invest. 1997; 100:18–24. [PubMed: 9202052]

4. Seko Y, Seko Y, Takahashi N, et al. Pulsatile stretch stimulates vascular endothelial growth factor (VEGF) secretion by cultured rat cardiac myocytes. Biochem Biophys Res Commun. 1999a; 254:462–465. [PubMed: 9918861]

5. Chang H, Wang BW, Kuan P, et al. Cyclical mechanical stretch enhances angiopoietin-2 and Tie2 receptor expression in cultured human umbilical vein endothelial cells. Clin Sci (Lond). 2003; 104:421–428. [PubMed: 12653688]

6. Cloutier M, Maltais F, Piedboeuf B. Increased distension stimulates distal capillary growth as well as expression of specific angiogenesis genes in fetal mouse lungs. Exp Lung Res. 2008; 34:101–113. [PubMed: 18307120]

7. Ingber DE, Prusty D, Sun Z, et al. Cell shape, cytoskeletal mechanics, and cell cycle control in angiogenesis. J Biomech. 1995; 28:1471–1484. [PubMed: 8666587]

8. Von Offenberg Sweeney N, Cummins PM, Cotter EJ, et al. Cyclic strain-mediated regulation of vascular endothelial cell migration and tube formation. Biochem Biophys Res Commun. 2005; 329:573–582. [PubMed: 15737624]

9. Pietramaggiori G, Liu P, Scherer SS, et al. Tensile Forces Stimulate Vascular Remodelling and Epidermal Cell Proliferation in Living Skin. Annals of Surgery. 2007; 246(5):896–902. [PubMed: 17968184]

10. Seko Y, Seko Y, Fujikura H, et al. Induction of vascular endothelial growth factor after application of mechanical stress to retinal pigment epithelium of the rat in vitro. Invest Ophthalmol Vis Sci. 1999b; 40:3287–3291. [PubMed: 10586955]

11. Shyu KG, Chang ML, Wang BW, et al. Cyclical mechanical stretching increases the expression of vascular endothelial growth factor in rat vascular smooth muscle cells. J Formos Med Assoc. 2001; 100:741–747. [PubMed: 11802532]

12. Saxena V, Orgill D, Kohane I. A set of genes previously implicated in the hypoxia response might be an important modulator in the rat ear tissue response to mechanical stretch. BMC Genomics. 2007; 8:430. [PubMed: 18034909]

13. Chin MS, Ogawa R, Lancerotto L, et al. In Vivo Acceleration of Skin Growth Using A Servo-Controlled Stretching Device. Tissue Eng Part C Methods. 2009a; 16(3):397–405. [PubMed: 19601702]

14. Fong GH. Regulation of angiogenesis by oxygen sensing mechanisms. J Mol Med. 2009; 87:549–560. [PubMed: 19288062]

15. Petersen W, Varoga D, Zantop T, et al. Cyclic strain influences the expression of the vascular endothelial growth factor (VEGF) and the hypoxia inducible factor 1 alpha (HIF-1alpha) in tendon fibroblasts. J Orthop Res. 2004; 22:847–853. [PubMed: 15183444]

16. Erba P, Ackermann M, Adini A, et al. Angiogenesis in Wounds Treated by Microdeformational Wound Therapy. Annals of Surgery. In press.

17. Chin MS, Lancerotto L, Helm DL, et al. Analysis of neuropeptides in stretched skin. Plast Reconstr Surg. 2009b; 124:102–113. [PubMed: 19568049]

18. Malkusch W, Konerding MA, Klapthor B, Bruch J. A simple and accurate method for 3-D measurements in microcorrosion casts illustrated with tumour vascularization. Anal Cell Pathol. 1995; 9(1):69–81. [PubMed: 7577757]

19. Zhong H, Simons JW. Direct comparison of GAPDH, beta-actin, cyclophilin, and 28S rRNA as internal standards for quantifying RNA levels under hypoxia. Biochem Biophys Res Commun. 1999; 259:523–526. [PubMed: 10364451]

20. Tonnesen MG, Feng X, Clark RA. Angiogenesis in wound healing. J Investig Dermatol Symp Proc. 2000; 5:40–46.

21. Manders EK, Schenden MJ, Furrey JA, et al. Soft-tissue expansion: concepts and complications. Plast Reconstr Surg. 1984; 74:493–507. [PubMed: 6484036]

22. Ilizarov GA. The tension-stress effect on the genesis and growth of tissues: Part II. The influence of the rate and frequency of distraction. Clin Orthop Relat Res. 1989:263–285. [PubMed: 2912628]

23. Gao JH, Ogawa R, Hyakusoku H, et al. Reconstruction of the face and neck scar contractures using staged transfer of expanded “Super-thin flaps”. Burns. 2007; 33:760–763. [PubMed: 17521819]

24. Borgquist O, Ingemansson R, Malmsjo M. Wound edge microvascular blood flow during negative-pressure wound therapy: examining the effects of pressures from −10 to −175 mmHg. Plast Reconstr Surg. 2010; 125:502–509. [PubMed: 20124835]

25. Gross MW, Karbach U, Groebe K, et al. Calibration of misonidazole labeling by simultaneous measurement of oxygen tension and labeling density in multicellular spheroids. Int J Cancer. 1995; 61:567–573. [PubMed: 7759162]

26. Raleigh JA, Chou SC, Arteel GE, et al. Comparisons among pimonidazole binding, oxygen electrode measurements, and radiation response in C3H mouse tumors. Radiat Res. 1999; 151:580–589. [PubMed: 10319731]

27. Haroon ZA, Raleigh JA, Greenberg CS, et al. Early wound healing exhibits cytokine surge without evidence of hypoxia. Ann Surg. 2000; 231:137–147. [PubMed: 10636114]

28. Albina JE, Mastrofrancesco B, Vessella JA, et al. HIF-1 expression in healing wounds: HIF-1alpha induction in primary inflammatory cells by TNF-alpha. Am J Physiol Cell Physiol. 2001; 281:1971–1977.

29. Morbidelli L, Birkenhaeger R, Roeckl W, et al. Distinct capillary density and progression promoted by vascular endothelial growth factor-A homodimers and heterodimers. Angiogenesis. 1997; 1(1):117–30. [PubMed: 14517398]

30. Potgens AJ, Lubsen NH, van Altena MC, et al. Covalent dimerization of vascular permeability factor/vascular endothelial growth factor is essential for its biological activity. Evidence from Cys to Ser mutations. J Biol Chem. 1994; 269(52):32879–85. [PubMed: 7806514]

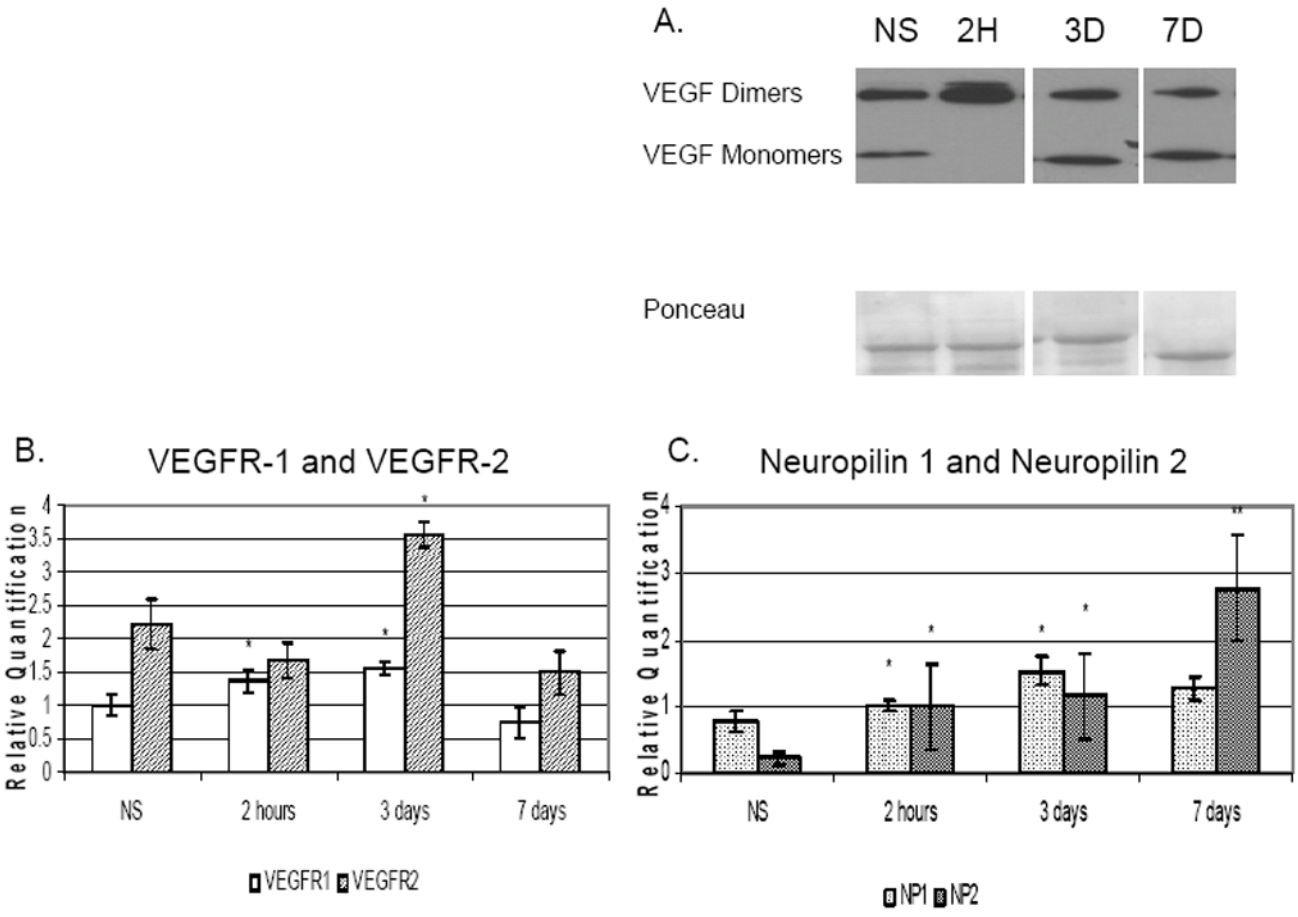

Figure 1.

A. Western Blot analysis of VEGF. Immediately after stretching VEGF monomers were reduced and VEGF dimers increased. VEGF protein level was slightly elevated starting 3 days after stretching. B and C. mRNA expression of VEGF receptors. While VEGFR1, VEGFR2 and NP1 showed only a moderate increase starting as early as 2 hours after stretching and reaching an expression peak at day 3, the expression of NP2 receptor presented with a 4 fold increase already 2 hours after stretching and reached a 12 fold of its original level at day 7. * $p<0.05$ compared to Non-Stretched. ** <0.01 compared to Non-Stretched.

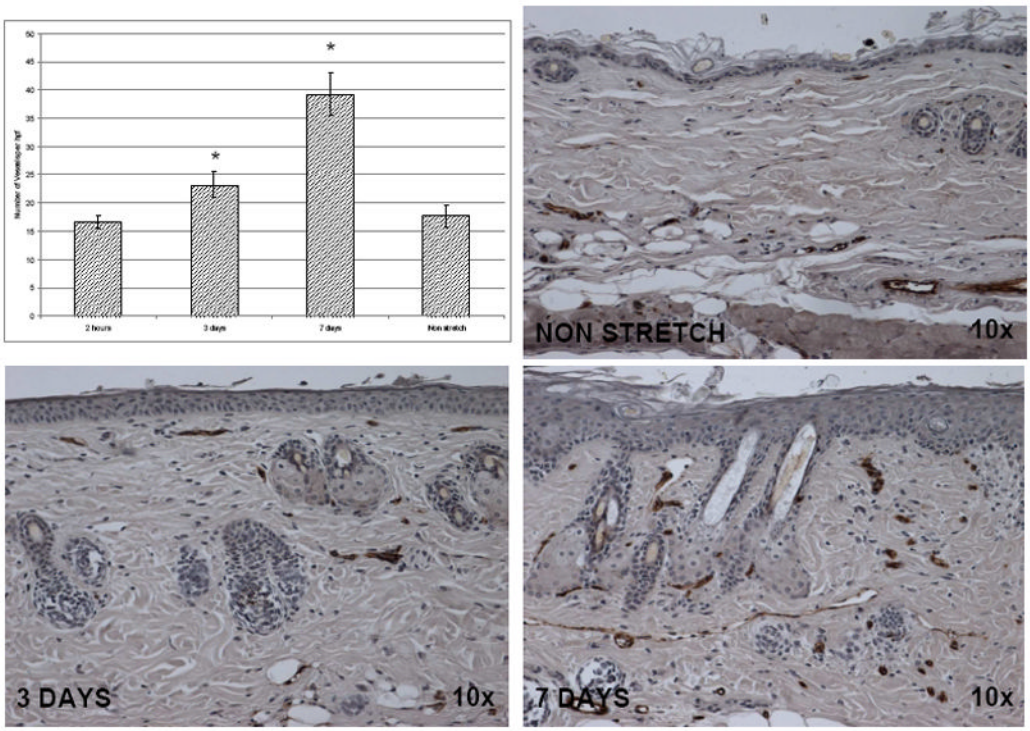

Figure 2.
CD-31 stained sections of stretched skin. Short lasting continuous skin stretching was able to induce a significant increase of the number of new vessels 3 days after stretching.

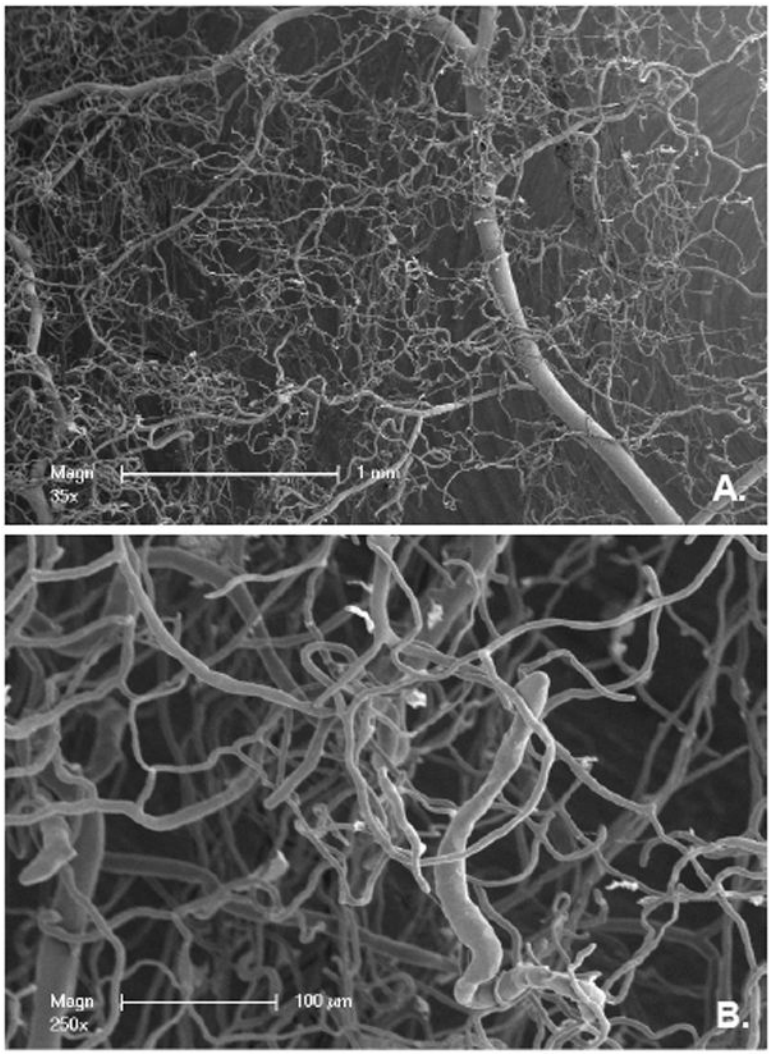

Figure 3.
Skin scanning electron micrographs of casted microvascular networks of control murine skin. (A) and (B) give some typical examples of non-stretched skin vasculature. Magnifications and scale bars indicated on the micrographs.

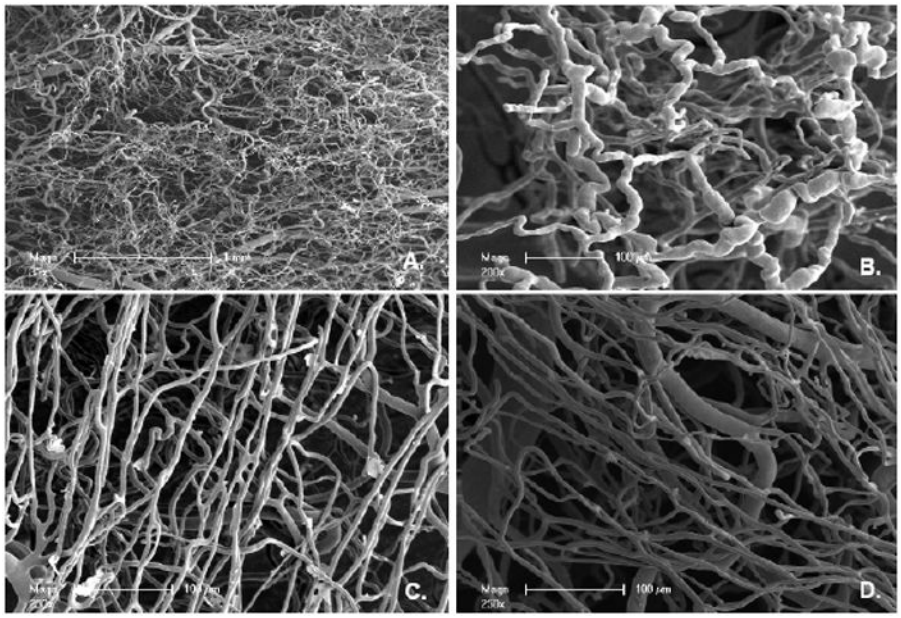

Figure 4.
Scanning electron micrographs of casted microvascular networks of murine skin after stretching. (A) and (B) give some typical examples of stretched skin vasculature. (A–B) show tortuous elongation of dilated vessel bundles that build transition zone of multidirectional vessel growth. (C–D) demonstrate densely packed thin vessels assuring optimal blood flow towards angiogenic transition zone. Magnifications and bars indicated on the micrographs.

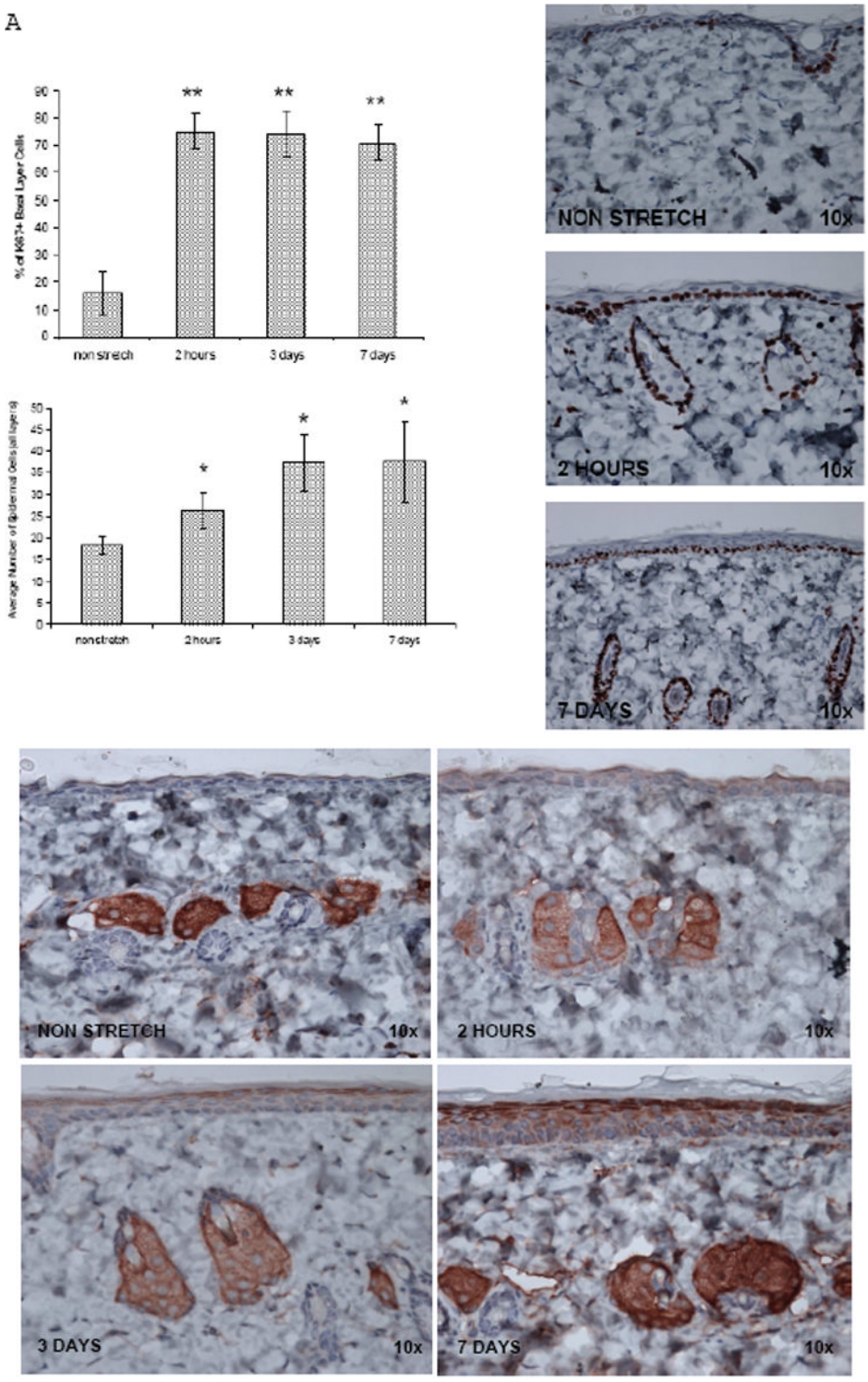

Figure 5.

A. Basal Cell proliferation is induced in stretched skin as early as 2 hours after application of tensile forces. While the percentage of proliferating cells remains constant over a 7 days observation period, the absolute number of proliferating cells increases over time and reaches a steady state after 3 days. * $p<0.05$ compared to Non-Stretched. ** <0.01 compared

to Non-Stretched. B. Pimonidazole Hydrochloride Staining of stretched mouse skin shows a progressive increase of hypoxic cells which are mainly located opposite to the proliferating basal cell layer, on the surface of the stretched epidermis. C. H&E staining of stretched skin shows an increasing number of epidermal cell layers. Epidermal changes appear already 2 hours after stretching.